Extinction coefficient of water-based multi-walled carbon nanotube nanofluids for application in direct-absorption solar collectors

Seung-Hyun Lee, Hyun Jin Kim, Kyu Han Kim, Seok Pil Jang

School of Aerospace and Mechanical Engineering, Korea Aerospace University, Goyang, Gyeonggi-do 412-791, Republic of Korea
E-mail: spjang@kau.ac.kr

Published in Micro & Nano Letters; Received on 15th May 2014; Accepted on 28th July 2014

In this reported work, the extinction coefficient of water-based nanofluids containing multi-walled carbon nanotubes (MWNCTs) has been experimentally measured. The MWCNTs were dispersed in deionised water with a surfactant, hexadecyltrimethyl-ammonium bromide, and they were homogenised by a bath-type ultrasonicator and a mechanical stirrer. The characteristics of MWCNTs suspended in the nanofluids were examined by transmission electron microscopy and scanning electron microscopy images and their hydrodynamic particle size was measured by a particle size analyser. The extinction coefficient of nanofluids was measured by an in-house developed apparatus at a single wavelength (632.8 nm) based on the Lambert-Beer principle. With the experimentally obtained extinction coefficient, the efficiency of a flat-plate type direct-absorption solar collector (DASC) was theoretically estimated. For this purpose, a modified analytical solution of the DASC efficiency is presented by assuming that the extinction coefficient is not a function of the wavelength. Finally, the efficiency of DASC is demonstrated according to the nanotube volume fractions. The results show that the DASC concept can further improve the efficiency of the conventional flat-plate type solar collectors.

1. Introduction: The most common types of solar thermal receivers today are surface-based absorbers, which are designed to capture solar thermal energy with the black-coloured metal plates [1]. However, the surface-based absorbers have limitations due to the high heat losses caused during the heat absorption and transfer processes [2, 3]. In particular, the surface absorbing approach is not appropriate to efficiently absorb the high radiant heat fluxes owing to the finite surface area [4]. To overcome this challenge, a direct-absorption solar collector (DASC) as a concept of the volumetric absorption approach was introduced [2–6]. Moreover, the nanofluids have significantly attracted interest as a working fluid of DASCs because of their excellent solar thermal energy absorption properties [2, 3, 7–9]. For example, Taylor *et al.* [7] have shown that the nanoparticles (graphite, copper, aluminium and silver) can significantly enhance the extinction coefficient of base fluids such as water and Therminol VP-1 at very low volume fractions below 0.001%. Lee and Jang [9] experimentally measured the extinction coefficient of water-based nanofluids containing multi-walled carbon nanotubes (MWCNTs) below 0.005 volume fractions. They also confirm that a small amount of nanotubes can significantly alter the extinction coefficient of deionised (DI)-water. On the basis of these, several researchers experimentally and numerically investigated the feasibility of the DASC using nanofluids and they showed that the efficiency of the DASC concept can further increase the efficiency of conventional solar collectors [2, 3, 5, 6]. To theoretically predict the efficiency of nanofluid-based DASCs, Veeraragavan *et al.* [10] developed analytical solutions for dimensionless temperature and DASC efficiency. However, their model is too complex to instinctively identify the important parameters of the efficiency of the DASC. In addition, they used theoretically obtained optical properties of nanofluids to estimate the dimensionless temperature field and the collector efficiency according to the magnitude of heat losses. In this Letter, water-based MWCNT nanofluids are prepared and their extinction coefficient is measured through the Lambert-Beer law. Moreover, we present a modified analytical solution of DASC efficiency by assuming that the extinction coefficient is not a strong function of the wavelength. Finally, we theoretically predict the efficiency of flat-plate type DASCs according to the volume fractions with the consideration of the experimentally obtained extinction coefficient. The presented results are also compared with the efficiency of the conventional flat-plate solar collectors.

2. Experimental study: Commercial MWCNTs were purchased from CNT Co. Ltd (Korea) and were dispersed in DI water with a surfactant, hexadecyltrimethyl-ammonium bromide (CTAB), about 0.25 wt%. To homogenise the mixture of MWCNTs and DI water, a mechanical stirrer was utilised for 15 min and a bath-type ultrasonicator for an hour, sequentially. Fig. 1 demonstrates the TEM and SEM images of MWCNTs. The results show that the tube length of the MWCNT is greater than 10 μm and the tube diameter is about 20–30 nm. The hydrodynamic size of the MWNCTs in nanofluids is about 53 nm, which is measured by a particle size analyser (Zetasiser Nano S 90, Malvern). The volume concentrations of the MWCNT nanofluids are 0.0005–0.005%. To measure the extinction coefficient of nanofluids, we used an in-house developed apparatus based on the Lambert-Beer law and its uncertainty is about 5% [9]. Fig. 2 shows the experimental results of the extinction coefficient and the correlation of the extinction coefficient is written as follows

$$K = 7610.374\,\varphi + 0.017 \quad (0.0005 < \varphi < 0.005\%,\ \lambda = 632.8\,\text{nm}) \tag{1}$$

where φ is the volume fraction of MWCNTs. Detailed characteristics of the nanofluids and the measurement system are shown in [9].

3. Analytical study: The governing equation and the boundary conditions of the DASC [5, 6, 10] are written as follows

$$\rho U c_p \frac{\partial T}{\partial x} = k_c \frac{\partial^2 T}{\partial y^2} + \dot{q}'''(y) \tag{2}$$

$$T|_{x=0} = T_{\text{in}};\quad \left.\frac{\partial T}{\partial y}\right|_{y=H} = 0;\quad k_c \left.\frac{\partial T}{\partial y}\right|_{y=0} = h_{\text{HL}}\left(T_{y=0} - T_{\text{amb}}\right) \tag{3}$$

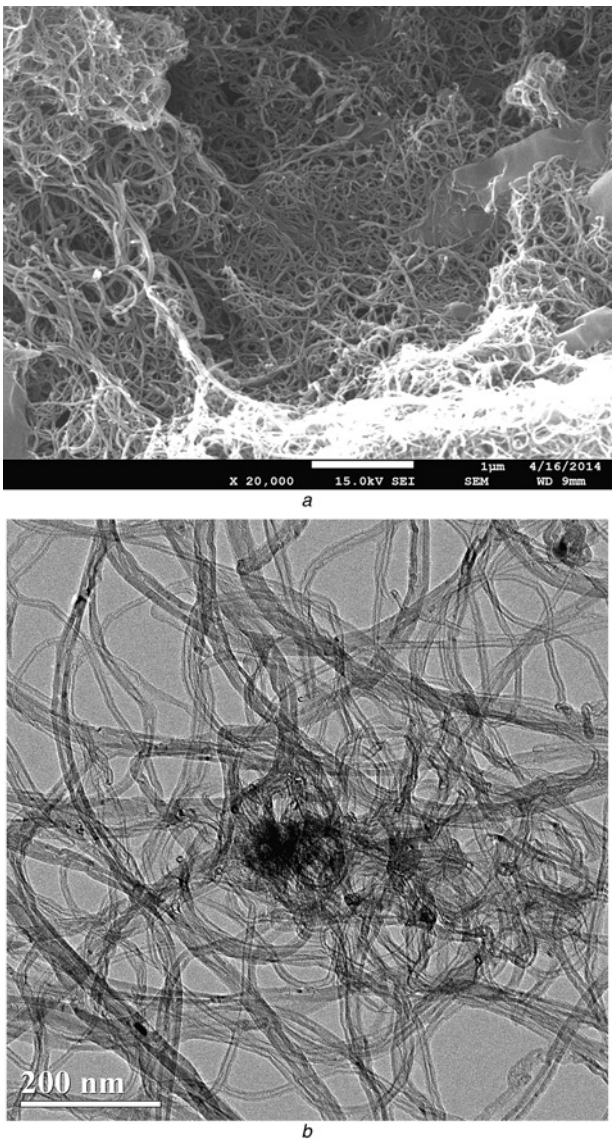

Figure 1 *SEM and TEM images of MWCNTs*
a SEM image
b TEM image

where c_p, h_{HL}, H, k_c, T, U and ρ are the specific heat of fluid, the convective heat loss coefficient, the receiver height, the thermal conductivity of fluid, the temperature, the fluid velocity and the density of fluid, respectively. $\dot{q}'''$ is the volumetric heat generation and the physical meaning is the absorbed solar radiation in a nanofluid. Subscripts amb, HL and in indicate ambient, heat loss and inlet, respectively. Fig. 3 shows a schematic of the analytical model of the nanofluid-based DASC. The non-dimensionalised parameters are given as follows [10]

$$\bar{y} = \frac{y}{H}; \quad \bar{x} = \frac{x}{\mathrm{Pe}H}; \quad \mathrm{Pe} = \mathrm{Re}\,\mathrm{Pr} = \frac{\rho U c_p H}{k_c}$$
$$\theta = \frac{k_c(T - T_{in})}{G_s H}; \quad \bar{q}''' = \frac{\dot{q}'''(y)H}{G_s}; \quad \mathrm{Nu} = \frac{h_{HL}H}{k_c} \tag{4}$$

where G_s, Nu, Pe, Pr, Re and θ are the incident solar heat flux at the Earth's surface (1368 W/m^2 = 1 Sun), the Nusselt number of heat loss, the Peclet number, the Reynolds number and the dimensionless temperature, respectively. With (4), the non-dimensionalised govern equation and boundary conditions

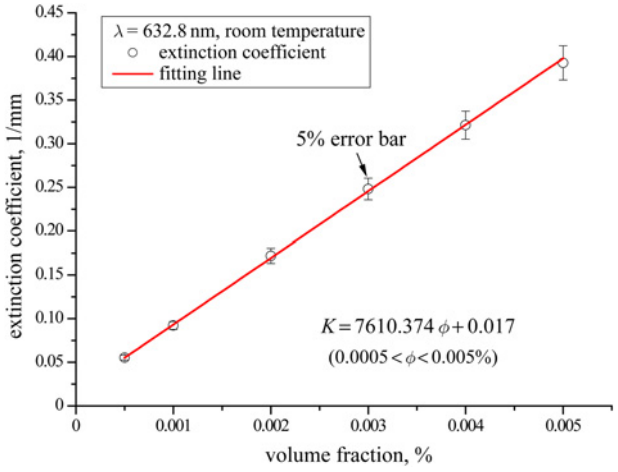

Figure 2 *Extinction coefficients of nanofluids and experimental correlation*

are expressed as follows

$$\frac{\partial\theta}{\partial\bar{x}} = \frac{\partial^2\theta}{\partial\bar{y}^2} + \bar{q}'''(\bar{y}) \tag{5}$$

$$\theta|_{x=0} = 0; \quad \left.\frac{\partial\theta}{\partial\bar{y}}\right|_{\bar{y}=1} = 0; \quad \left.\frac{\partial\theta}{\partial\bar{y}}\right|_{\bar{y}=0} = \mathrm{Nu}(\theta_{\bar{y}=0} - \theta_{amb}) \tag{6}$$

where θ_{amb} is zero. The heat generation profile in the nanofluid is determined by a radiative transport equation (RTE). The RTE is given as follows:

$$\frac{\mathrm{d}I_\lambda}{\mathrm{d}y} = -K_\lambda I_\lambda \tag{7}$$

where I_λ, K_λ and λ indicate the spectral intensity, the spectral extinction coefficient and the wavelength. The spectral intensity is obtained by solving ordinary differential (7)

$$I_\lambda(y) = I_{0,\lambda}\mathrm{e}^{-K_\lambda y} \tag{8}$$

where $I_{0,\lambda}$ represents the incident spectral intensity at $y = 0$. Thus, the volumetric heat generation profile is expressed as follows with respect to the y-direction

$$\dot{q}'''(y) = -\frac{\mathrm{d}}{\mathrm{d}y}\int_0^\infty I_\lambda(y)\,\mathrm{d}\lambda = -\frac{\mathrm{d}}{\mathrm{d}y}\int_0^\infty (I_{0,\lambda}\cdot \mathrm{e}^{-K_\lambda y})\,\mathrm{d}\lambda \tag{9}$$

In this equation, we assume that the extinction coefficients of nanofluids are nearly independent of wavelength. Since this assumption is satisfied when the nanofluid is very dilute [11,12], we can utilise this assumption because the volume fraction range is very low (<0.015%). Thus, the volumetric heat generation

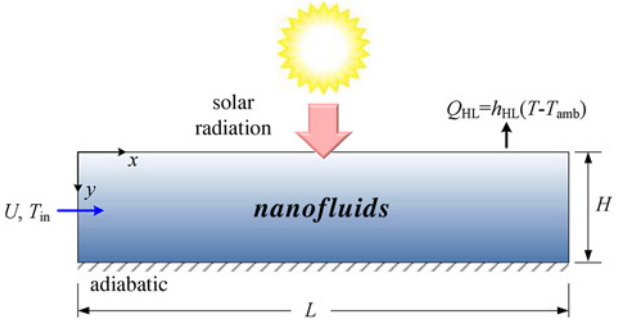

Figure 3 *Schematic of the theoretical model of DASC*

doi: 10.1049/mnl.2014.0262

profile and its dimensionless form are obtained as follows

$$\dot{q}'''(y) = K\exp(-Ky)G_s \tag{10}$$

$$\bar{\dot{q}}'''(\bar{y}) = HK\exp(-HK\bar{y}) \tag{11}$$

With the above assumption, a general solution of the governing equation is written as follows

$$\theta = \theta_h + \theta_p = \sum_{n=1}^{\infty} A_n e^{-\alpha_n^2\bar{x}} Y_n(\bar{y}) + \int_0^1 G(\bar{y},\,\xi)\bar{q}'''(\xi)\,\mathrm{d}\xi \tag{12}$$

with

$$Y_n(\bar{y}) = \frac{\cos(\alpha_n(\bar{y}-1))}{\sin\alpha_n}, \qquad Z = \frac{\theta_{\mathrm{amb}}}{\int_0^1 \bar{q}'''(\xi)d\xi} \sim 0$$

$$G(\bar{y},\,\xi) = \begin{cases} G^-(\bar{y},\,\xi) = \dfrac{1}{\mathrm{Nu}} + \xi + Z; & (0 \le \xi \le \bar{y}) \\ G^+(\bar{y},\,\xi) = \dfrac{1}{\mathrm{Nu}} + \bar{y} + Z; & (1 \ge \xi \ge \bar{y}) \end{cases}$$

$$A_n = \frac{-\int_0^1 \left[\left(\int_0^1 G(\bar{y},\,\xi)\bar{q}'''(\xi)\mathrm{d}\xi\right)Y_n(\bar{y})\right]\mathrm{d}\bar{y}}{\int_0^1 Y_n^2(\bar{y})\mathrm{d}\bar{y}}$$

where $G(\bar{y},\,\xi)$, Y_n, Z, α_n and ξ are the Green function, the eigenfunction, the constant to satisfy the boundary condition of a particular solution, the eigenvalues to satisfy a relationship ($\mathrm{Nu}/\alpha_n = \sin\alpha_n/\cos\alpha_n$) and the location of a source for the Green function. The detailed derivation procedure was developed in [10]. By substituting (11) into (12), a closed form of dimensionless temperature is obtained as follows:

$$\theta = \left[C_1 - \frac{1}{\tau\exp(\tau\bar{y})} - \frac{\bar{y}}{\exp(\tau)}\right] + \sum_{n=1}^{20}\frac{A_n}{\exp(\alpha_n^2\bar{x})}\frac{\cos(\alpha_n(\bar{y}-1))}{\sin(\alpha_n)} \tag{13}$$

$$A_n = \sum_{n=1}^{20}\frac{4\alpha_n\cdot\sin\alpha_n}{\{2\alpha_n+\sin(2\alpha_n)\}}\left[-\frac{C_1\cdot\sin\alpha_n}{\alpha_n} + \frac{1-\cos\alpha_n}{\alpha_n^2\cdot\exp(\tau)} + \frac{1}{\tau^2+\alpha_n^2}\left(\frac{\alpha_n\cdot\sin\alpha_n}{\tau} + \cos\alpha_n - \frac{1}{\exp(\tau)}\right)\right]$$

with

$$C_1 = \left[\frac{1}{\mathrm{Nu}} + \frac{1}{\tau} + Z - \left(\frac{1}{\mathrm{Nu}} + Z\right)\exp(-\tau)\right]$$

where τ is the optical thickness ($\tau = HK$). To show the validity of the presented solution, the dimensionless temperature profile is depicted in Fig. 4 with the previous results [10]. Fig. 4*a* indicates that the temperature profile of the presented modified solution (for $H = 7.9$ mm, $K = 1.0359\ \mathrm{mm}^{-1}$ and $\mathrm{Nu} = 1$) is well matched with the previous exact solution [10]. Moreover, as shown in Fig. 4*b*, the shape and trend are similar with the temperature field of Veeraragavan *et al.* [10]. From the definition of the collector efficiency, the dimensionless form of collector efficiency is derived as follows [10]

$$\eta = \frac{\dot{m}c_p(T_{\mathrm{out}} - T_{\mathrm{in}})}{AG_s} = \frac{\int_0^1 \theta(\bar{L},\,\bar{y})\mathrm{d}\bar{y}}{\bar{L}}$$

$$\eta = \left(\frac{\mathrm{Pe}}{\mathrm{AR}}\right)\left[C_1 + \frac{1}{\tau^2}\left(\frac{1}{\exp(\tau)} - 1\right) - \frac{1}{2\exp(\tau)}\right] + \sum_{n=1}^{20}\frac{4\cdot\mathrm{Pe}\cdot\sin(\alpha_n)}{\{2\alpha_{\mathrm{PF},n}+\sin(2\alpha_n)\}\mathrm{AR}}\exp\left(\frac{-\alpha_n^2\mathrm{AR}}{\mathrm{Pe}}\right) \times\left[-\frac{C_1\cdot\sin\alpha_n}{\alpha_n} + \frac{1-\cos\alpha_n}{\alpha_n^2\cdot\exp(\tau)} + \frac{1}{\tau^2+\alpha_n^2}\left\{\frac{\alpha_n\cdot\sin\alpha_n}{\tau} + \cos\alpha_n - \frac{1}{\exp(\tau)}\right\}\right] \tag{14}$$

where $\mathrm{AR} = L/H$ is the aspect ratio and $\bar{L}$ is the dimensionless length of the receiver. As described in (14), the important parameters of DASC efficiency are the height of the receiver (H), the extinction coefficient of the fluid (K), the magnitude of heat loss (Nu), the Peclet number of the fluid (Pe) and the length of the receiver (L). In particular, the extinction coefficient is the key factor in improving DASC efficiency under fixed DASC geometries and flow conditions.

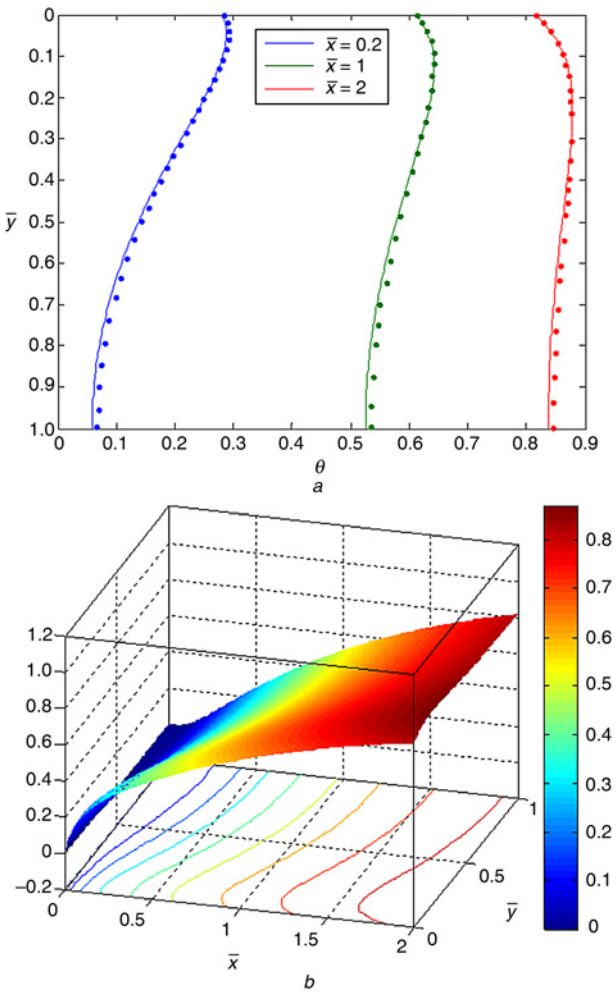

Figure 4 *Validation results of present modified analytical solution*
a Temperature profile with respect to the *y*-direction (lines: presented results, points: Veeraragavan *et al.* [10])
b Temperature field in the DASC

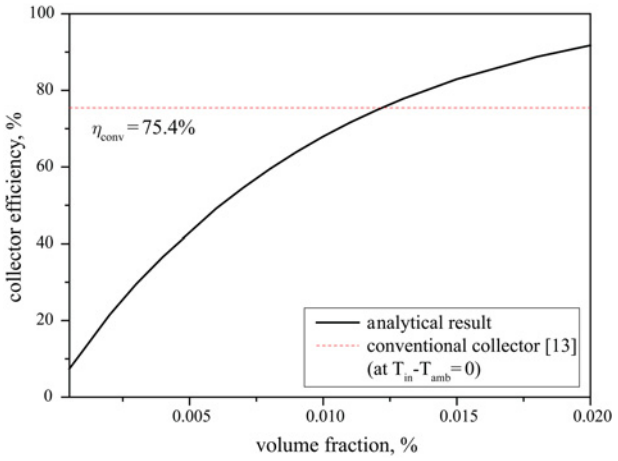

Figure 5 *Analytical result of the DASC efficiency with respect to nanotube volume concentrations*

4. Results and discussion: With the extinction coefficient correlation and modified analytical solution, the efficiency of flat-plate type DASC using nanofluids can be predicted under the given geometries and flow conditions [5]. Fig. 5 shows the efficiency of the flat-plate type NVR increases with the increase of the volume fractions (or the extinction coefficients) of water-based MWCNT nanofluids. The crossover point beyond the conventional collector's efficiency is about 0.012 vol.%. This means that if we use a dense nanofluid more than 0.012 vol%, better efficiency can be achieved without using the conventional absorbing metal plates. Although the presented receiver's geometry ($L = 1$ m [5]) is somewhat different from the actual dimensions of the conventional receiver (W 0.84 m × L 1.9 m) [13], it should be enough to show the feasibility of the NVR. Moreover, based on the presented analytical solutions, researchers can simply predict the temperature field and efficiency of the DASC with only consideration of the extinction coefficient of nanofluids. In other words, when we measure the extinction coefficient of nanofluids, the DASC efficiency can be easily predicted according to the various geometrical and flow conditions.

5. Conclusion: In this reported work, we prepared water-based MWCNTs using the two-step method and measured the extinction coefficient of nanofluids. The MWCNTs suspended in nanofluids are characterised by TEM and SEM images, and a particle size analyser. The extinction coefficient of nanofluids was measured by in-house developed apparatus with 5% uncertainty at a wavelength of 632.8 nm. Moreover, the closed form of the modified analytical solutions of the DASC efficiency and the temperature field are presented by assuming that the extinction coefficient of nanofluid is not a function of the wavelength. Finally, the efficiency of the DASC is demonstrated according to the nanotube volume fractions. The results show that the DASC concept can further improve the efficiency of conventional flat-plate type solar collectors. The results of this work may be helpful to simply predict receiver efficiency with greater ease as well as to design the NVRs.

6. Acknowledgments: This work was supported by the Defense Acquisition Program Administration and the Agency for Defense Development contract UD120030ID.

7 References

[1] Kalogirou S.A.: 'Solar thermal collectors and applications', *Prog. Energy Combust. Sci.*, 2004, **30**, (3), pp. 231–295
[2] Otanicar T.P., Phelan P.E., Prasher R.S., Rosengarten G., Taylor R.A.: 'Nanofluid-based direct absorption solar collector', *J. Renewable Sustainable Energy*, 2010, **2**, (3), p. 033102
[3] Lenert A., Wang E.N.: 'Optimization of nanofluid volumetric receivers for solar thermal energy conversion', *Sol. Energy*, 2012, **86**, (1), pp. 253–265
[4] Miller F.J., Koenigsdorff R.W.: 'Thermal modeling of a small-particle solar central receiver', *J. Sol. Energy Eng. – ASME*, 2000, **122**, (1), pp. 23–29
[5] Tyagi H., Phelan P., Prasher R.: 'Predicted efficiency of a low-temperature nanofluid-based direct absorption solar collector', *J. Sol. Energy Eng. – ASME*, 2009, **131**, (4), p. 041004
[6] Taylor R.A., Phelan P.E., Otanicar T.P., *ET AL.*: 'Applicability of nanofluids in high flux solar collectors', *J. Renewable Sustainable Energy*, 2011, **3**, (2), p. 023104
[7] Taylor R.A., Phelan P.E., Otanicar T.P., Adrian R., Prasher R.: 'Nanofluid optical property characterization: towards efficient direct absorption solar collectors', *Nanosc. Res. Lett.*, 2011, **6**, (1), p. 225
[8] Mercatelli L., Sani E., Zaccanti G., *ET AL.*: 'Absorption and scattering properties of carbon nanohorn-based nanofluids for direct sunlight absorbers', *Nanosc. Res. Lett.*, 2011, **6**, (1), p. 282
[9] Lee S.-H., Jang S.P.: 'Extinction coefficient of aqueous nanofluids containing multi-walled carbon nanotubes', *Int. J. Heat Mass. Transfer*, 2013, **67**, pp. 930–935
[10] Veeraragavan A., Lenert A., Yilbas B., Al-Dini S., Wang E.N.: 'Analytical model for the design of volumetric solar flow receivers', *Int. J. Heat Mass Transfer*, 2012, **55**, (4), pp. 556–564
[11] Sani E., Barison S., Pagura C., *ET AL.*: 'Carbon nanohorns-based nanofluids as direct sunlight absorbers', *Opt. Express*, 2010, **18**, (5), pp. 5179–5187
[12] Gan Y., Qiao L.: 'Optical properties and radiation-enhanced evaporation of nanofluid fuels containing carbon-based nanostructures', *Energy Fules*, 2012, **26**, (7), pp. 4224–4230
[13] Streed E.R., Hill J.E., Thomas W.C., Dawson A.G., Wood B.D.: 'Results and analysis of a round robin test program for liquid-heating flat-plate solar collectors', *Sol. Energy*, 1979, **22**, (3), pp. 235–249

doi: 10.1049/mnl.2014.0262